

Highlights

Sensor-fusion based Prognostics Framework for Complex Engineering Systems Exhibiting Multiple Failure Modes

Benjamin Peters, Ayush Mohanty, Xiaolei Fang, Stephen K. Robinson, Nagi Gebraeel

- We propose a two-stage prognostic framework for multi-sensor systems with multiple failure modes.
- **Offline:** An unsupervised method labels failure events and ranks sensor importance.
- **Online:** Sensor features are fused for failure mode diagnosis, then key sensors predict RUL.
- Our method achieves 80% clustering accuracy and $< 3\%$ RUL prediction error in simulations.
- In NASA turbofan data, early predictions outperform benchmarks while reducing input by 30%.

Sensor-fusion based Prognostics Framework for Complex Engineering Systems Exhibiting Multiple Failure Modes

Benjamin Peters^a, Ayush Mohanty^{b,*}, Xiaolei Fang^c, Stephen K. Robinson^d,
Nagi Gebraeel^b

^a*Manufacturing and Industrial Engineering, University of Texas at Rio Grande
Valley, Edinburg, 78539, TX, United States of America*

^b*School of Industrial & Systems Engineering, Georgia Institute of
Technology, Atlanta, 30332, GA, United States of America*

^c*Department of Industrial and Systems Engineering, North Carolina State
University, Raleigh, 27607, NC, United States of America*

^d*Department of Mechanical and Aerospace Engineering, University of California
Davis, Davis, 95616, CA, United States of America*

Abstract

Complex engineering systems are often subject to multiple failure modes. Developing a remaining useful life (RUL) prediction model that does not consider the failure mode causing degradation is likely to result in inaccurate predictions. However, distinguishing between causes of failure without manually inspecting the system is nontrivial. This challenge is increased when the causes of historically observed failures are unknown. Sensors, which are useful for monitoring the state-of-health of systems, can also be used for distinguishing between multiple failure modes as the presence of multiple failure modes results in discriminatory behavior of the sensor signals. When systems are equipped with multiple sensors, some sensors may exhibit behavior correlated with degradation, while other sensors do not. Furthermore, which sensors exhibit this behavior may differ for each failure mode. In this paper, we present a simultaneous clustering and sensor selection approach for unlabeled training datasets of systems exhibiting multiple failure modes. The cluster assignments and the selected sensors are then utilized in real-time to first diagnose the active failure mode and then to predict the system RUL. We validate the methodology using a simulated dataset of systems exhibiting two failure modes and on NASA turbofan degradation dataset.

*Corresponding Author, ayush.mohanty@gatech.edu

Keywords: Multiple Failure Modes, Remaining Useful Life, Sensor Fusion, Functional Principal Component Analysis, Mixture of Gaussian Regression, Adaptive Sparse Group Lasso, Expectation Maximization

1. Introduction

Prognostic models aim to estimate the remaining useful life (RUL) of critical components and systems. They are important because they drive condition-based maintenance decisions that aim to increase equipment availability, reduce downtime, and prevent unexpected failures. Generally, prognostic models can be classified into two categories: (1) data-driven models that focus on modeling sensor data and assume that the data is directly (or indirectly) correlated with the underlying physical degradation process, and (2) physics-based models that rely on first principles and require a thorough understanding of the underlying physics driving the degradation process. While physics-based approaches are known for their high accuracy, data-driven approaches are growing in popularity, especially for modeling complex systems. Several reasons are driving this trend. First, complex systems often exhibit complex physics of failure that are difficult to characterize using first principles. The second reason is the rise of Machine Learning and Artificial Intelligence models, which when trained properly can be very powerful prognostic tools. However, many data-driven prognostics models assume that complex systems exhibit a single predominant failure mode that can be used to accurately predict the system's RUL. In practice, complex engineering systems often exhibit multiple failure modes and thus require more sophisticated modeling approaches to account for the different ways/modes a system can fail.

In this paper, we focus on developing a prognostic methodology for complex systems monitored by multiple sensors that exhibit multiple failure modes. We design an integrated framework comprised of (1) a sensor selection algorithm, (2) a dimensionality reduction and data fusion methodology, and (3) a RUL prediction model. Our methodology relies on a historical dataset to simultaneously diagnose observed failure events and select the subset of the most informative sensors associated with each failure mode. One of the unique aspects of our methodology relates to the sensor selection model, which uses an unsupervised approach to identify the dominant failure modes. **Unlike most of the existing works, we assume that the labels of the**

failure events are unknown a priori. This assumption introduces some unique challenges around model estimation. These challenges are not trivial, especially when they are considered in conjunction with sensor selection.

Our methodology is comprised of two parts, an offline component and an online prognostic model. In the offline part, we develop a novel algorithm based on the Expectation-Maximization (EM) algorithm that simultaneously labels the failures in the historical training set and selects the optimal sensors for each failure mode. In the online part, we utilize real-time data to perform online diagnosis of the predominant failure mode and RUL prediction. During the online learning phase, Multivariate Functional Principle Component Analysis (MFPCA) is utilized for feature extraction and dimensionality reduction. We then use the nearest neighbor classifier to diagnose the active failure mode in the real-time signals before fitting a weighted functional regression model using the extracted features. The main contributions of this paper are threefold:

- First, we propose a *feature extraction* methodology comprised of fusing signals from multiple sensors originating from a set of systems exhibiting multiple failure modes.
- Second, we propose an optimization methodology for simultaneous failure mode labeling and sensor selection for any given unlabeled historical dataset. We call this as the “*offline sensor selection*” step.
- Finally, we provide a two-step sequential approach to leverage this knowledge of failure labels and informative sensors to (1) perform active failure mode diagnosis and (2) subsequent RUL prediction on systems degrading in real-time. The paper mentions this as the “*online diagnosis and prognostics*” step.

The remainder of the paper is outlined as follows. In Section 2, we review the relevant literature associated with this research area. In Section III, we outline our proposed multi-failure mode prognostics framework. In Section 4, we present our offline sensor selection scheme that utilizes an EM algorithm. In Section 5, we present our online diagnostics and prognostics method. It discusses a strategy to fuse informative sensors for real-time diagnosis of failure modes and subsequent prediction of RUL. Our methodology is demonstrated through two case studies – one using a simulated dataset in section 6 and the other NASA turbofan engine dataset in section 7. We conclude by summarizing our framework and key findings in Section 8.

2. Literature Review

Data-driven prognostic models utilize a variety of approaches. A significant number of these rely on Artificial Intelligence tools, such as neural networks to predict component lifetime [1, 2]. Some approaches have focused on directly modeling degradation-based signals that are derived from raw sensor data. Examples include random coefficient models [3], relevance vector machines [4], stochastic processes such as the Brownian motion process [5], the Gamma process [6], and hidden Markov models [7], and similarity-based prognostic models [8]. Most of these models have been developed for modeling a single sensor or degradation-based signal. Extending these approaches to applications involving multiple sensors is not straightforward.

Fusion algorithms have been leveraged to model multivariate sensor data. According to [9], fusion is usually performed at the decision level or the data level. Decision-based fusion involves combining the results of multiple prediction models in an ensemble fashion [10]. Conversely, data fusion methodologies focus on aggregating data from multiple sensors to develop a single (univariate) health index, which can then be modeled using the conventional methods discussed above. Most of the works in this area are characterized by their data fusion approach. Examples include principal component analysis (PCA) [11, 12, 13], maximum likelihood [14], deep learning [15], and state space models [16, 17, 18]. Most data fusion methodologies tend to aggregate all the sensor data. In practice, some sensors may not be correlated with the underlying failure process. Thus, integrating signals from these sensors into a data fusion algorithm introduces noise and may impact RUL prediction accuracy. To address this issue, several works have incorporated sensor selection algorithms. For example, [14] and [9] employed adaptive lasso to penalize non-informative sensors. [13] combined location-scale regression with group regularization technique to perform sensor selection. While these techniques can select an optimal subset of sensors for monitoring, they still assume that system failure is caused by a single predominant failure mode.

Most complex engineering systems can fail due to multiple failure modes. Competing risk models have been a popular approach for modeling multiple failure modes. Traditionally, competing risk models rely on statistical approaches. For example, [19] uses the Cox proportional hazard model (PHM) [20] with the Weibull baseline hazard rate to develop a mixture of Weibull PHM. For an extensive review of statistical competing risk models, we refer the reader to [21]. Deep learning has also been used to develop competing

risk models. These models include convolutional neural network (CNN) [22], recurrent neural networks [23], and LSTM [24]. Recently, [25] developed a deep learning methodology to model complex survival problems, such as recurrent hospitalizations due to kidney failure or pancreas graft. For more examples, we refer the reader to [26], which provides a review of machine learning methodologies for survival analysis. Competing risk models often output survival/hazard rates that are sometimes difficult to interpret in engineering applications. Consequently, many researchers have adopted methods that explicitly model sensor data to predict RUL.

The literature that focuses explicitly on RUL prediction of systems with multiple failure models can be loosely divided into two groups. The first group uses deep learning approaches while the second group utilizes more statistical methods. Deep learning models such as [27] and [28] develop feature extraction methodologies based on convolutional neural networks (CNN) for modeling systems with multiple failure modes. [29] developed a Gaussian model whose mean is a Bayesian deep neural network that maps sensor data to the RUL. In [30], the authors used a support vector machine to diagnose the active failure mode using features extracted from a deep belief network. Following diagnosis, a particle filter is employed to predict RUL. [31] trained an LSTM-based RUL prediction model for all present failure modes. The choice of prediction model is based on a deep CNN-based classifier trained with physics-informed failure labels. While deep learning approaches have been successful at predicting RUL, their parameters are often difficult to interpret. Additionally, they require significantly larger datasets for training compared to statistical methods. In [32], the authors derived a composite health index for each failure mode and used a random coefficients-based polynomial degradation model to predict the system’s RUL. In their model training/estimation, the authors assumed that the labels of the failure modes were given. In fact, this assumption has been widely used in the literature and is often supported by visual inspection of the data [27, 30, 32] or available domain knowledge [31]. [33] assumes that a subset of the data is labeled and utilizes a similarity-based approach for classifying the rest of the unlabeled failure modes in the training set.

Our methodology differs from previous works in that we consider a scenario where the failure labels are completely unknown. Furthermore, we assume that for each failure mode, there exists a (not necessarily disjoint) subset of informative sensors that are useful for prognostics. Our objective is to design an unsupervised prognostic methodology that synthesizes signals

from multiple sensors in a systematic fashion. We assume the availability of a historical repository of system failures whose degradation was monitored from the moment an incipient fault occurred up to system failure using multiple sensors. The methodology assumes that all systems fail independently of each other. In addition, we assume that only one type of failure mode can occur in the entire lifetime of the system. While the failure labels are unknown, the total number of potential failure modes for the system is assumed to be known.

3. Overview of the Prognostics Framework

This section describes our multiple failure mode prognostics framework, which is summarized in the flowchart in Figure 1. This framework is comprised of two parts:

Offline Sensor Selection: The first part is performed offline and primarily focuses on utilizing a training set of *historically observed degradation signals* to perform sensor selection. Sensor selection is important because not all sensors are informative for prognostics, and the inclusion of non-informative sensors in a prognostics algorithm can compromise the accuracy of RUL predictions. When performing sensor selection, it is computationally convenient to represent each sensor by a parsimonious set of features that capture the system dynamics. Therefore we further divide this step into the following substeps:

1. **Feature Extraction:** It involves a variant of the traditional Functional Principal Component Analysis (FPCA) framework to account for multiple failure modes in the unlabeled data.
2. **Optimization:** This involves formulating an optimization model to simultaneously label the failure modes and select the informative sensors for each failure mode.

Feature Extraction: There are many ways to extract parsimonious features from complex and multivariate data. In our framework, we choose to use a Functional Principal Component Analysis (FPCA) framework due to its flexibility and extensibility to various types of functional data, allowing us to efficiently capture the underlying patterns and variability in complex, high-dimensional datasets. FPCA models the variability of temporal data observations around a mean function. However, the presence of multiple

failure modes can cause heterogeneity in the magnitude and/or sign of the signals' rate of change, compromising the effectiveness of FPCA as a prognostic tool. Therefore, the first step of our offline sensor selection algorithm is to extract features using a Covariate-Adjusted FPCA (CA-FPCA) approach [34].

CA-FPCA is an extension of conventional FPCA that allows modeling functional data while accounting for the effects of explanatory variables, known as *covariates*. In our context, **the covariates are used to represent the failure modes**. One of the unique contributions of our approach is the assumption that the failure modes are not known a priori. However, CA-FPCA assumes that covariates are observable. We note that the way each sensor responds to different failure modes can be highly variable. For example, a sensor may be more sensitive to one failure mode than another resulting in heterogeneity in the rate of change of its corresponding sensor signals. Furthermore, a sensor signal may increase in magnitude in response to one failure mode, and decrease for another. To address the lack of observable covariates, we first perform regular FPCA on the signals from each sensor. Then, we perform K-means clustering on the FPC scores for each sensor individually, using the resulting cluster labels as the covariate values to perform CA-FPCA.

Optimization: After feature extraction the sensor signals are transformed into parsimonious CA-FPC-scores, which serve as predictors for a Mixture of Gaussian (MGR) model used to model the natural logarithm of the time-to-failure, $\ln TTF$, as a function of the CA-FPC-scores. This model is motivated by the assumption that the functional relationship between the $\ln TTF$ and the CA-FPC scores is dependent on the latent failure mode. We fit the parameters of the MGR model using the Expectation-Maximization (EM) algorithm. In the E-step, we obtain a soft clustering of the (CA-FPC-scores, $\ln TTF$) tuples into their respective failure modes. In the M-step, we incorporate the Adaptive Sparse Group Lasso (ASGL) penalty into the regression model to remove groups of features associated with non-informative sensors. From now on, we refer to this model as MGR-ASGL. The output of the offline sensor selection step of our methodology are (1) failure mode labels for each sample in the training set and (2) a subset of informative sensors for each failure mode.

Online diagnosis and Prognostics: The second part of our methodology consists of an online step used to process and analyze data from units operating in the field. The online step consists of diagnosing the active fail-

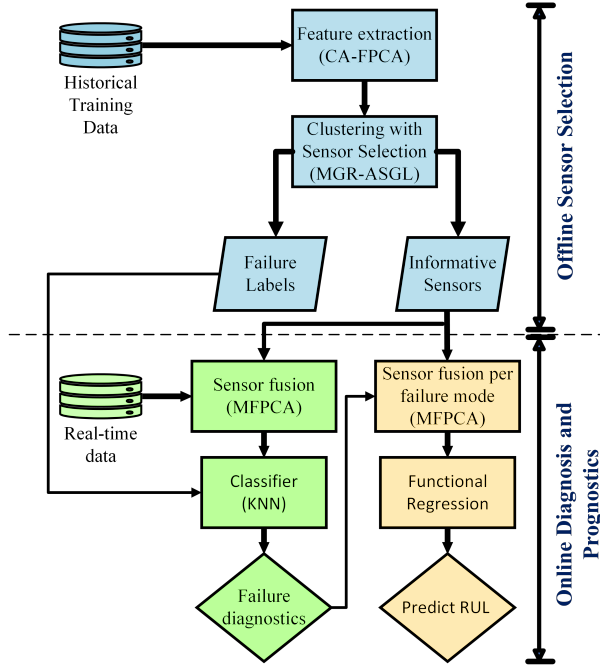


Figure 1: Flowchart of the multiple failure mode prognostics framework

ure mode of the fielded unit and then predicting the RUL of the fielded unit. In the diagnostic step, features are extracted from the *real-time data* generated by all selected sensors using Multivariate FPCA (MFPCA), which is an extension of FPCA to multivariate functional data. We use MFPCA to generate a parsimonious set of fused signal features from multivariate sensor signals; hereafter referred to as MFPC-scores. Then, we classify the active failure mode of the fielded unit by assigning to the unit the failure mode most frequently represented by its K -nearest neighbors. Once this step is complete, we recalculate the MFPC scores using only the informative sensors associated with the diagnosed failure mode of the unit. In the prognostic step, we fit a functional regression model using the MFPC scores that predict the RUL of the unit. In the following sections, we formalize our prognostics framework.

4. Offline Sensor Selection Algorithm

We consider a scenario where a system is monitored by P sensors. We assume there exists a historical dataset comprised of P -dimensional degradation-

based sensor signals from monitoring N similar systems. We denote $s_{i,p}(t)$ as the signal data from sensor $p \in \{1, \dots, P\}$ for system $i \in \{1, \dots, N\}$ observed at time $t \in [0, T]$, where $T = \min(\{TTF_i\}_{i=1}^N)$. By truncating all signals to the minimum failure time, we ensure that all signals in the training set have the same time domain and that they are all included when modeling. For this framework, we assume that the total number of failure modes, K is known, but that the actual failure modes in the training dataset are unknown. This poses a challenge for CA-FPCA, which requires observed covariates for computation. To determine these covariates, we perform a sensor-wise clustering of the training samples. For each sensor, we perform FPCA for feature extraction and then use K-means clustering with K clusters to label the signals from that sensor. Once the sensor-wise clustering is complete, the next step involves feature extraction by applying CA-FPCA and then regressing these features against the time-to-failure to identify the most informative subset of sensors for each failure mode. The next two subsections discuss details about CA-FPCA and the penalized Mixture of Gaussian regression model (MGR-ASGL).

4.1. Feature Extraction: CA-FPCA

CA-FPCA extends conventional FPCA to handle complex data structures where the dynamics of time-varying signals are affected by one or more additional factors, i.e. covariates. In [34], the covariates are assumed to be continuous variables, and thus, mean and covariance estimation requires smoothing over both time and the covariate space. In this paper, **we use the sensor-wise cluster labels as covariates**. Let \mathcal{I}_p^k denote the set of indices for sensor p signals assigned to cluster $k, k \in \{1, 2, \dots, K\}$. The CA-FPCA problem was reduced to performing FPCA on each cluster. For a given system i , signals from cluster k of sensor p are modeled as:

$$s_{i,p}(t) = v_{i,p}^k(t) + \epsilon_{i,p}(t), i \in \mathcal{I}_k^p \quad (1)$$

where $v_{i,p}^k(t)$ is a smooth random function, and $\epsilon_{i,p}(t)$ are assumed to be independently and identically distributed (i.i.d.) errors with mean zero and variance ς_p^2 . $v_{i,p}^k(t)$ and $\epsilon_{i,p}(t)$ are assumed to be independent of each other. The mean and covariance functions of $v_{i,p}^k(t)$ are given by $\mu_p^k(t)$ and $\mathbb{C}_p^k(t, t')$, respectively. Using Mercer's theorem [35], the covariance can be decomposed as follows, $\mathbb{C}_p^k(t, t') = \sum_{m=1}^{\infty} \lambda_{m,p}^k \phi_{m,p}^k(t) \phi_{m,p}^k(t')$, where $\{\phi_{m,p}^k(t)\}_{m=1}^{\infty}$ are the orthogonal eigenfunctions of $\mathbb{C}_p^k(t, t')$ and $\lambda_{1,p}^k \geq \dots \geq \lambda_{m,p}^k \geq \dots$ are the

corresponding eigenvalues. By projecting the mean-subtracted signal data onto the eigenfunctions, we can represent the signals by equation (2).

$$s_{i,p}(t) = \mu_p^k(t) + \sum_{m=1}^{\infty} \xi_{i,m,p}^k \phi_{m,p}^k(t) + \epsilon_{i,p}(t) \quad (2)$$

where $\xi_{i,m,p}^k$ is the m th CA-FPC-score with mean 0 and variance $\lambda_{m,p}^k$. The CA-FPC scores are computed using the PACE algorithm in [36]. Since the eigenvalues decrease as $m \rightarrow \infty$, we can obtain a low-dimensional representation of $s_{i,p}^k(t)$ using the first q_p CA-FPC-scores.

To ensure all features are scaled equally, we use the standardized versions of the CA-FPC-scores: $x_{i,m}^p = \frac{\sum_{k=1}^K \xi_{i,m,p}^k \mathbb{I}(i \in \mathcal{I}_p^k)}{\sqrt{\frac{1}{N-1} \sum_{k=1}^{r_p^*} N_p^k \lambda_{m,p}^k}}$, where N_p^k is the number of signals assigned to cluster k for sensor p . We extract $\mathbf{x}_{i,p} = (x_{i,1}^p, \dots, x_{i,q_p}^p)^T$ for sensor p of system i . We then utilize this *boldsymbol* $x_{i,p}$'s as predictors for fitting the MGR-ASGL model.

4.2. Optimization of the MGR-ASGL model

To perform sensor selection, we seek to model the distribution of $\ln TTF$ conditioned on the observed set of features. In what follows, we note that values of $\ln TTF$ are standardized. Our modeling approach assumes that the failure times are conditionally independent given the observed features. Let y_i denote the random variable corresponding to the $\ln TTF$ of the system i . We consider \mathbf{Z}_i to denote a ‘‘one-hot’’ random vector of length K , where $\mathbf{Z}_i[k] = 1$ if system i failed due to failure mode k , and zero otherwise. For mathematical brevity, we let $\mathbf{Y} = (y_1, \dots, y_N)$ denote the observed $\ln TTF$ and $\mathbb{Z} = (\mathbf{Z}_1, \mathbf{Z}_2, \dots, \mathbf{Z}_N)$ denote the set of random vectors representing the failure modes for each system. In the following subsections, we first assign probability distributions to these random variables to formalize the MGR model. Second, we construct the log-likelihood function for the MGR model. Third, we provide theoretical intuition on the use of the EM algorithm for model fitting. Fourth, we describe the ASGL penalty. Finally, we provide details for implementing the EM algorithm.

4.2.1. Mixture of Gaussian Regression (MGR) model

We assume that the distribution of y_i conditioned on the observed features $\{\mathbf{x}_{i,1}, \dots, \mathbf{x}_{i,p}\}$ and $\mathbf{Z}_i[k] = 1$ is Gaussian. If we let π_1, \dots, π_K , where $\sum_{k=1}^K \pi_k = 1$, denote the mixing coefficients, which represent the probability

that $\mathbf{Z}_i[k] = 1$ ($\forall k = \{1, \dots, K\}$), then equation (3) gives the marginal distribution of y_i given only $\{\mathbf{x}_{i,1}, \dots, \mathbf{x}_{i,p}\}$. This marginal distribution is the MGR model.

$$f_{\vartheta}(y_i | \mathbf{x}_{i,1}, \dots, \mathbf{x}_{i,P}) = \sum_{k=1}^K \pi_k \frac{1}{\sqrt{2\pi}\sigma_k} \times \exp \left(-\frac{1}{2\sigma_k^2} \left(y_i - \beta_{0,k} - \sum_{p=1}^P \mathbf{x}_{i,p}^T \boldsymbol{\beta}_{p,k} \right)^2 \right) \quad (3)$$

4.2.2. Log-Likelihood

Utilizing the strategy mentioned in [37], we can achieve a scale-invariant form of the MGR model by introducing $\rho_k = 1/\sigma_k$, $\psi_{0,k} = \beta_{0,k}/\sigma_k$ and $\boldsymbol{\psi}_{p,k} = \boldsymbol{\beta}_{p,k}/\sigma_k$. Let $\boldsymbol{\Pi}$ denote the set $\{\pi_1, \dots, \pi_K\}$, $\boldsymbol{\rho} = \{\rho_1, \dots, \rho_K\}$ and $\boldsymbol{\Psi} = \{\boldsymbol{\psi}_{p,k} : \forall p = 0, \dots, P \ \& \ \forall k = 1, \dots, K\}$. We define superset $\boldsymbol{\Theta} = \{\boldsymbol{\Pi}, \boldsymbol{\rho}, \boldsymbol{\Psi}\}$ to be the set of parameters for the MGR model. In what follows, we formally define the log-likelihood for when the true failure labels are unknown (Definition 1) and known (Definition 2).

Definition 1. The log-likelihood function for the MGR model is given by equation (4). This function is called as the "incomplete-data log-likelihood" (IDLL), since we do not know the cause of the observed failure in the data.

$$\ell(\boldsymbol{\Theta}; \mathbf{Y}) = \sum_{i=1}^N \ln \sum_{k=1}^K \pi_k \times \frac{\rho_k}{\sqrt{2\pi}} \exp \left(-\frac{1}{2} \left(\rho_k y_i - \psi_{0,k} - \sum_{p=1}^P \mathbf{x}_{i,p}^T \boldsymbol{\psi}_{p,k} \right)^2 \right) \quad (4)$$

Definition 2. The "complete-data log-likelihood" (CDLL) given by equation (5) assumes knowledge of the underlying causes of the observed failure in the data.

$$\ell_C(\boldsymbol{\Theta}; \mathbf{Y}, \mathbf{Z}) = \sum_{i=1}^N \sum_{k=1}^K \mathbf{Z}_i[k] \ln \pi_k \left(\frac{\rho_k}{\sqrt{2\pi}} \right) \exp \left(-\frac{1}{2} \left(\rho_k y_i - \psi_{0,k} - \sum_{p=1}^P \mathbf{x}_{i,p}^T \boldsymbol{\psi}_{p,k} \right)^2 \right) \quad (5)$$

The IDLL given in equation (4) is difficult to optimize globally [38]. Instead, we search for a local optimum by using EM algorithm, an iterative algorithm suitable for fitting probability models with latent variables. To derive the steps of the EM algorithm, we note that since $\ln(\cdot)$ is a concave

Algorithm 1: Offline Sensor Selection Algorithm

Input : Number of systems N , Number of sensors P , Unlabeled data from P sensors of all N systems, Maximum iterations $iter_{max}$ for EM algorithm, threshold δ for regression coefficient's l_2 -norm

Output: Vector \mathbf{Z} indicating failure labels, Set of informative sensors \mathcal{P}_k for each failure mode k

```

/* Feature Extraction from all  $P$  sensors (CA-FPCA) */
1 for  $p = 1$  to  $P$  do
2    $\mathcal{I}_k^p \leftarrow$  K-means clustering on FPC-scores;
3   for  $k = 1$  to  $K$  do
4      $\xi_{i,m,p}(k) \leftarrow$  Use  $\mathcal{I}_k^p$  to obtain CA-FPC-scores (Eq. 2);
5   end
6    $x_{i,p} \leftarrow$  Obtain standardized CA-FPC-scores;
7    $q_p \leftarrow$  Number of CA-FPC-scores retained for sensor  $p$ ;
8 end
/* MGR-ASGL based EM algorithm */
9 Initialize  $\mathcal{P}_k \leftarrow \emptyset \forall k$ ,  $\Psi^0 \leftarrow 0$ ,  $\Pi^0 \sim \text{Uniform}(K)$ ,  $\boldsymbol{\rho}^0 \leftarrow \text{randint}$ 
    $iter \leftarrow 0$ ;
10 while  $iter \leq iter_{max}$  do
11    $\gamma_i^{iter} \leftarrow$  Use  $x_{i,p}$  in Eq. (7) for all  $i$ ; ; // E-step
12    $\Pi^{iter} \leftarrow$  Update using Eq. (9); ; // M-step for  $\Pi$ 
13    $\boldsymbol{\rho}^{iter}, \Psi^{iter} \leftarrow$  Solve Eq. (8) using  $\sum_{p=1}^P \sqrt{q_p}$  and  $\gamma_i^{iter}$ ;
14    $iter \leftarrow iter + 1$ ;
15 end
16  $\gamma_i^{iter_{max}} \leftarrow$  Final responsibilities from Eq. (7);
17  $\mathbf{Z}_i[\arg \max_k \gamma_i^{iter_{max}}] \leftarrow 1$  for all  $i$ ;
18  $\mathbf{Z}_i[\sim \arg \max_k \gamma_i^{iter_{max}}] \leftarrow 0$  for all  $i$ ;
19 foreach  $p$  and  $k$  do
20   if  $\|\psi_{p,k}^{iter_{max}}\|_2 \geq \delta$  then
21     Append  $p$  to  $\mathcal{P}_k$ ; // Significant sensors for failure
     mode  $k$ 
22   ;
23 end
24 end

```

function We use Jensen's inequality to form a lower bound on the IDLL. This lower bound is the expectation of the CDLL given in equation (5) and shown in Lemma 1.

Lemma 1. *The expectation of the CDLL w.r.t distribution g is a lower bound for the IDLL i.e.,*

$$\mathbb{E}_g [\ell_C(\Theta; \mathbf{Y}, \mathbb{Z})] \leq \ell(\Theta; \mathbf{Y})$$

Proof. Let g be an arbitrary distribution on $\mathbf{Z}_i[k]$. Then we can re-write equation (4) as follows:

$$\ell(\Theta; \mathbf{Y}) = \sum_{i=1}^N \ln \left(\sum_{k=1}^K \frac{g(\mathbf{Z}_i[k]) p(y_i, \mathbf{Z}_i[k]; \Theta)}{g(\mathbf{Z}_i[k])} \right)$$

where,

$$\begin{aligned} & p(y_i, \mathbf{Z}_i[k]; \Theta) \\ &= \pi_k \cdot \left(\frac{\rho_k}{\sqrt{2\pi}} \exp \left(-\frac{1}{2} \left(\rho_k y_i - \psi_{0,k} - \sum_{p=1}^P \mathbf{x}_{i,p}^T \boldsymbol{\psi}_{p,k} \right)^2 \right) \right) \end{aligned}$$

Since $\ln(\cdot)$ is concave, from Jensen's inequality we can write that,

$$\ell(\Theta; \mathbf{Y}) \geq \sum_{i=1}^N \sum_{k=1}^K g(\mathbf{Z}_i[k]) \ln \frac{p(y_i, \mathbf{Z}_i[k]; \Theta)}{g(\mathbf{Z}_i[k])}$$

and thus,

$$\ell(\Theta; \mathbf{Y}) \geq \mathbb{E}_g [\ell_C(\Theta; \mathbf{Y}, \mathbb{Z})] - \sum_{i=1}^N \sum_{k=1}^K g(\mathbf{Z}_i[k]) \ln g(\mathbf{Z}_i[k])$$

The second term on the right side of the inequality is the negative entropy of the g distribution. Since it is positive, the inequality holds. \square

For every iteration of the EM algorithm, the E-step calculates the conditional expectation of the CDLL given the observed failure times, which we denote as $\mathbb{E}_{\Theta_{\text{old}}}[\ell_C(\Theta; \mathbf{Y}, \mathbb{Z})|\mathbf{Y}]$. In the M-step, we find the parameters that maximize the conditional expectation (see equation (8)). The parameter estimation equations of the EM algorithm are provided in III.B.5.

4.2.3. Adaptive Sparse Group Lasso (ASGL) penalty

The inclusion of features from non-informative sensors can negatively impact the accuracy of the RUL prediction. To address this issue, we penalize the negative-scaled conditional expectation of the CDLL function using the Adaptive Sparse Group Lasso (ASGL) penalty to obtain the following minimization problem given by 6.

$$\min_{\Theta} -\frac{1}{N} \mathbb{E}_{\Theta_{\text{old}}} [\ell_C(\Theta; \mathbf{Y}, \mathbb{Z}) | \mathbf{Y}] + \lambda \sum_{k=1}^K \pi_k \sum_{p=1}^P \sqrt{q_p} \times [(1 - \alpha) \|\boldsymbol{\psi}_{p,k}\|_2 + \alpha \|\boldsymbol{\psi}_{p,k}\|_1] \quad (6)$$

ASGL is an extension of lasso [39] that ensures the coefficients for all features of a non-informative group (sensor) are reduced to zero. In the context of regularization, adaptive refers to the penalty accounting for the number of CA-FPC-scores retained for each sensor i.e., q_p , and the mixing coefficient for each failure mode i.e., π_k . While the inclusion of q_p ensures a sensor is not retained simply by having more coefficients, π_k accounts for the class imbalance. $\lambda > 0$ and $\alpha \in [0, 1]$ are the hyperparameters for this model.

4.2.4. Expectation Maximization algorithm

We now describe the EM algorithm used to find a local optimum to the IDLL described. Given an initial estimate of the model parameters Θ_{old} , we perform the E-step and M-step as follows:

E-step: The E-step consists of computing the expectation of CDLL in (6) conditioned on \mathbf{Y} . Let $\mathcal{Q}(\Theta | \Theta_{\text{old}}) = -\mathbb{E}_{\Theta_{\text{old}}} [\ell_C(\Theta; \mathbf{Y}, \mathbb{Z}) | \mathbf{Y}]$ denote the negative expectation of the CDLL. In order to compute $\mathcal{Q}(\Theta | \Theta_{\text{old}})$, we need to compute $\gamma_{i,k} = \mathbb{E}_{\Theta_{\text{old}}} [Z_i[k] | \mathbf{Y}]$, which represents the responsibility of failure mode k to system i and is given by equation (7). For any system i , we denote the vector of the responsibilities $\gamma_{i,k}$ across all failure modes as $\boldsymbol{\gamma}_i$ such that, $\boldsymbol{\gamma}_i = \{\gamma_{i,1}, \dots, \gamma_{i,K}\}$.

$$\gamma_{i,k} = \frac{\pi_k^{\text{old}} \rho_k^{\text{old}} \times \exp\left(-\frac{1}{2} \left(\rho_k^{\text{old}} y_i - \psi_{0,k}^{\text{old}} - \sum_{p=1}^P \mathbf{x}_{i,p}^T \boldsymbol{\psi}_{p,k}^{\text{old}}\right)^2\right)}{\sum_{l=1}^K \pi_l^{\text{old}} \rho_l^{\text{old}} \exp\left(-\frac{1}{2} \left(\rho_l^{\text{old}} y_i - \psi_{0,l}^{\text{old}} - \sum_{p=1}^P \mathbf{x}_{i,p}^T \boldsymbol{\psi}_{p,l}^{\text{old}}\right)^2\right)} \quad (7)$$

M-Step: During the M-step, we update the parameters by solving the opti-

mization problem in (8) with respect to Θ .

$$\min_{\Theta} \frac{1}{N} Q(\Theta | \Theta_{\text{old}}) + \lambda \sum_{k=1}^K \pi_k \sum_{p=1}^P \sqrt{q_p} \times [(1 - \alpha) \|\psi_{p,k}\|_2 + \alpha \|\psi_{p,k}\|_1] \quad (8)$$

Improvement with respect to Π : To update the mixing coefficients, we set $\rho_k = \rho_k^{\text{old}}$, $\psi_{0,k} = \psi_{0,k}^{\text{old}}$, $\psi_{p,k} = \psi_{p,k}^{\text{old}}$ and solve optimization problem (8). We utilize the update strategy from [37]. We start by identifying a feasible solution $\bar{\Pi}^{\text{new}} = \left(\frac{1}{N} \sum_{i=1}^N \gamma_{i,1}, \dots, \frac{1}{N} \sum_{i=1}^N \gamma_{i,K} \right)^T$ and then update the mixing coefficients as described by equation (9), where $t^{\text{new}} \in (0, 1]$ is chosen to be the largest value in $\{0.1^k; k = 0, 1, 2, \dots\}$ such that the objective function does not increase.

$$\Pi^{\text{new}} = \Pi^{\text{old}} + t^{\text{new}} (\bar{\Pi}^{\text{new}} - \Pi^{\text{old}}) \quad (9)$$

Improvement with respect to ρ and Ψ : For this, we utilize the updated mixing coefficients Π^{new} of the previous step. Since the ρ_k 's and $\psi_{p,k}$'s are independent for each failure mode, the expression in (8) decouples into K distinct optimization problems. Once the estimators ρ_k^{new} , $\psi_{0,k}^{\text{new}}$, and $\psi_{p,k}^{\text{new}}$ are determined, they are used to update the cluster responsibilities in the E-step.

After the EM algorithm is completed, we obtain optimal Π , ρ , and, Ψ . We substitute these optimal values to equation (7) to obtain the responsibilities γ_i 's. For each pair of sensor data and failure time, we assign the failure mode with the largest responsibility. This results in class labels for the training set. To perform sensor selection for failure mode k , we compute $\|\psi_{p,k}\|_2$, the l_2 -norm of the regression coefficients for sensor p and failure mode k . We deem a sensor informative for failure mode k if the l_2 -norm of its regression coefficients is greater than 0.001. The detailed step-wise implementation of the offline sensor selection step is given in algorithm 1.

5. Online diagnosis and Prognostics

This section details the steps of the online part of our multi-failure mode prognostics framework. In this part, a fielded unit is degrading in real-time, and our goal is to predict the time remaining before the unit fails. We begin by showing how MFPCA is used to fuse the signals from multiple sensors into a parsimonious set of features. Then, we demonstrate how we utilize MFPCA to i) diagnose the active failure mode of the degrading unit, in real-time, and ii) predict its RUL.

Algorithm 2: Online Diagnosis and Prognostics

Input : Smoothed signals from training & test units, Failure labels of training data from Algorithm 1, Set of informative sensors \mathcal{P}_k from Algorithm 1

Output: Active failure mode in the test unit k^* , Remaining Useful Life (RUL) of the test unit RUL_{test}

```
/* Diagnostic Model Training */
1  $\zeta_{(i),h} \leftarrow$  MFPCA on training units (Eq. 10);
2 Train a KNN classifier using  $\zeta_{(i),h}$ ;

/* Diagnostic Model Testing */
3  $\zeta_{test,h} \leftarrow$  MFPCA on test unit;
4  $k^* \leftarrow$  Mode of labels in KNN of  $\zeta_{test,h}$ ;

/* Prognostic Model Training */
5  $\zeta_{(i),h}^{k^*} \leftarrow$  MFPCA: selected sensors (Eq. 14);
6  $c_0^{k^*}, \dots, c_h^{k^*} \leftarrow$  Obtain arg min in Eq. 17;

/* Prognostic Model Testing */
7  $\zeta_{test,h}^{k^*} \leftarrow$  MFPCA on test unit (Eq. 14);
8  $RUL_{test} \leftarrow$  Equation 18;
```

5.1. Sensor Fusion: MFPCA

Without loss of generality, let us redefine the sensor index as $\{1, 2, \dots, \mathcal{P}\}$, where \mathcal{P} is number of sensors we seek to fuse. Now assume that we have monitored an online unit (operating in the field) for a duration given by the time interval $[0, t^*]$. Since we are interested in predicting the remaining lifetime, we only use signals from units with failure times greater than t^* . We define this set as the “ t^* -training” set, whose indices we denote by the set \mathcal{I}_{t^*} , which has cardinality N_{t^*} . Furthermore, we smooth the degradation signals using the ‘rloess’ method as described in [40]. This method uses weighted least squares with a 2nd-order polynomial for smoothing. The weights come from a bisquare weight function requiring a specified bandwidth parameter. This method also identifies outliers and assigns them weights of zero to improve signal mean estimation. To perform MFPCA, we model the i th smoothed multivariate signal evaluated at time t as $\mathbf{s}_i(t) = \mathbf{u}_i(t) + \boldsymbol{\epsilon}_i(t)$, where $\mathbf{u}_i(t) \in \mathcal{R}^{\mathcal{P}}$ is a random multivariate function with mean $\boldsymbol{\mu}(t)$ and covariance function $\mathcal{C}(t, t')$, $\boldsymbol{\epsilon}_i(t) \in \mathcal{R}^{\mathcal{P}}$, and $t \in [0, t^*]$ are i.i.d. zero-mean

error vectors with covariance Σ_ϵ . We assume $\mathbf{u}_i(t)$ and $\epsilon_i(t)$ are independent of each other. Using the first H multivariate eigenfunctions, we can represent the multivariate signal by equation 10 where the MFPC-scores ζ 's are computed according to equation 11.

$$\mathbf{s}_i(t) = \boldsymbol{\mu}(t) + \sum_{h=1}^H \zeta_{i,h} \boldsymbol{\varpi}_h(t) + \epsilon_i(t), \quad (10)$$

$$\zeta_{i,h} = \int_0^{t^*} (\mathbf{s}_i(t) - \boldsymbol{\mu}(t))^T \boldsymbol{\varpi}_h(t) dt \quad (11)$$

5.2. Failure Mode Diagnosis: K -nearest Neighbors

In order to diagnose the failure mode of a degrading unit at time t^* , we apply MFPCA on the t^* training dataset. Next, K nearest neighbors (KNN) is applied to the extracted MFPC scores to identify the active failure mode. Here, the distance metric of the KNN classifier is defined using the Euclidean distance between the MFPC scores. Given this diagnosis, we now develop a model for predicting the unit RUL.

5.3. RUL Prediction: Weighted Functional Regression

To predict RUL, we use a weighted time-varying functional regression model that maps multivariate signal features to the $\ln TTF$. First, we discuss the basics of a time-varying functional regression and then motivate the case for a weighted version of the model

5.3.1. Time-Varying Functional Regression

When predicting RUL, we are often faced with updating the relationship between time-to-failure and the current values of the extracted signal features (FPC scores). The predictor trajectories up to the current time are represented by time-varying FPC scores, which are continuously updated as time progresses and are considered to be time-varying predictor variables for the functional regression model. This is referred to as *time-varying functional regression*. It was first proposed by [41] and has been used for prognostics in [42, 13].

In our problem setting, let k^* denote the diagnosed failure mode and $\mathcal{I}_{t^*}^{k^*} \subset \mathcal{I}_{t^*}$ denote the set of indices for training units that failed due to failure mode k^* , but survived up to time t^* . Furthermore, let $\mathcal{P}_{k^*} \subset \{1, 2, \dots, \mathcal{P}\}$ denote the set of sensors selected (identified as most informative) for failure mode k^* . To predict RUL, we fit a functional regression model using least

squares as shown in equation (12), where $y_i = \ln TTF_i$, $\varphi_0^{k^*}$ is the bias term, $\boldsymbol{\varphi}^{k^*}(t) \in \mathcal{R}^{|\mathcal{P}_{k^*}|}$ is the multivariate coefficient function, and $\mathbf{s}_i^{k^*}(t)$ is the multivariate signal consisting only of sensors significant to failure mode k^* .

$$\min_{\varphi_0^{k^*}, \boldsymbol{\varphi}^{k^*}(t)} \sum_{i \in \mathcal{I}_{t^*}^{k^*}} \left(y_i - \varphi_0 - \int_0^{t^*} \boldsymbol{\varphi}^{k^*}(t)^T \mathbf{s}_i^{k^*}(t) dt \right)^2 \quad (12)$$

We expand the coefficient function using the eigenfunctions obtained from applying MFPCA on the training set $\mathcal{I}_{t^*}^{k^*}$. The regression coefficient function can now be expanded as shown in equation (13), where H_{k^*} denotes the number of MFPC-scores that were retained for failure mode k^* .

$$\boldsymbol{\varphi}(t) = \sum_{h=1}^{H_{k^*}} c_h^{k^*} \boldsymbol{\varpi}_h^{k^*}(t) \quad (13)$$

Likewise, we expand the multivariate signals using the eigenfunctions as shown in equation (14).

$$\mathbf{s}_i^{k^*}(t) = \boldsymbol{\mu}^{k^*}(t) + \sum_{h=1}^{H_{k^*}} \zeta_{i,h}^{k^*} \boldsymbol{\varpi}_h^{k^*}(t) \quad (14)$$

Since the eigenfunctions are orthogonal, substituting equations (13) and (14) into equation (12) yields the following optimization problem,

$$\min_{c_0^{k^*}, c_1^{k^*}, \dots, c_{H_{k^*}}^{k^*}} \sum_{i \in \mathcal{I}_{t^*}^{k^*}} \left(y_i - c_0^{k^*} - \sum_{h=1}^{H_{k^*}} \zeta_{i,h}^{k^*} c_h^{k^*} \right)^2 \quad (15)$$

where,

$$c_0^{k^*} = \varphi_0^{k^*} + \int_0^{t^*} \sum_{h=1}^{H_{k^*}} c_h^{k^*} \boldsymbol{\varpi}_h^{k^*}(t)^T \boldsymbol{\mu}^{k^*}(t) \quad (16)$$

Weighted Version: We note that the offline sensor selection algorithm may generate some outliers, which can impact the accuracy of the regression problem. These outliers become more apparent after identifying the active failure mode and the MFPC scores to estimate the time-varying functional regression model. To address this issue, we use weighted least squares to estimate the time-varying functional regression mode. To derive the weights, we first measure the Euclidean distance between the MFPC score corresponding to a unit i and the centroid of the cluster of the active failure mode. We then use the reciprocal of that distance to define the corresponding weight

for the unit, w_i , of that unit. If the unit's failure is misclassified, w_i would be large, and thus, unit i is assigned a smaller weight in the regression problem. Next, We regress the $\ln TTF$ on the MFPC scores using a weighted linear regression shown in equation (17). The solution to this problem can be found using weighted least squares regression [43]. For variable selection, we include the lasso penalty in the optimization problem.

$$\min_{c_0^{k^*}, c_1^{k^*}, \dots, c_{H_{k^*}}^{k^*}} \sum_{i \in \mathcal{I}_t^{k^*}} \left(\sqrt{w_i} y_i - \sqrt{w_i} c_0^{k^*} - \sum_{h=1}^{H_{k^*}} \sqrt{w_i} \zeta_{i,h}^{k^*} c_h^{k^*} \right)^2 + \lambda \sum_{h=1}^{H_{k^*}} \|c_h^{k^*}\| \quad (17)$$

5.3.2. RUL prediction

As we have shown, MFPCA enables the transformation of the functional regression problem to a multiple linear regression problem, which enables us to solve the problem only by estimating $H_{k^*} + 1$ parameters. After fitting the regression coefficients, we extract the MFPC scores for the test signal $\zeta_{test,1}^{k^*}, \dots, \zeta_{test,H_{k^*}}^{k^*}$. These scores are then used to predict the RUL at time t^* using equation (18).

$$RUL_{test} = \exp \left(c_0^{k^*} + \sum_{k=1}^{H_{k^*}} \zeta_{test,h}^{k^*} c_k^{k^*} \right) - t^* \quad (18)$$

6. Case Study 1: Simulated Dataset

We present a case study using a simulated data set to evaluate the performance of our methodology in terms of its ability to cluster the training data, effectiveness in selecting informative sensors for each failure mode, and accuracy in predicting the RUL. Furthermore, we test the robustness of our methodology to varying degrees of signal noise. In section VI-A, we describe the simulation model. In section VI-B, we display the simulated data and evaluate the performance of the MGR-ASGL model at clustering and sensor selection. Finally, we evaluate the prediction accuracy of our online prognostics approach in section VI-C.

6.1. Simulation Model

We utilize a modified version of the simulation model used in [13] to generate degradation signals for a set of engineering systems. We assume that each system is monitored by 20 sensors and exhibits one of two possible

failure modes that we refer to as failure mode 1 (FM 1) and failure mode 2 (FM 2). We generate data for 200 systems for each failure mode. Out of the 200 systems, we use 160 systems for model training and 40 systems for testing model performance. The simulated data consists of the sensor signals for each system and the corresponding failure time, which is utilized later as the ground truth to evaluate prediction accuracy.

The signals of the underlying degradation process for system i exhibiting failure mode k are generated according to equation (19). The signal is parameterized by the random coefficient $\theta_i^k \sim N(\mu_k, 0.1^2)$, which is used to control the degradation rate. We let $\mu_1 = 1$, and $\mu_2 = 0.8$ be the degradation rates for FM 1 and FM 2, respectively. The TTF is computed as the first time the degradation signal $s_i^k(t)$ crosses a soft failure threshold D_k . We set the failure thresholds for FM 1 and FM 2 as $D_1 = 2$ and $D_2 = 1.5$, respectively.

$$s_i^k(t) = -\frac{\theta_i^k}{\ln t} \quad (19)$$

This paragraph describes the procedure for simulating degradation signals for each sensor. Here we consider a practical scenario where only a subset of sensors is correlated with the underlying degradation process associated with a given failure mode. These sensors are the informative sensors and their signal trends reflect the severity and progression of the degradation process. Note that sensors that do not exhibit any consistent trends leading up to a failure event are deemed noninformative. We define \mathcal{J}_k as the index set of informative sensors for failure mode k , and \mathcal{N}_k as the set of noninformative sensors such that $\mathcal{N}_k \cap \mathcal{J}_k = \{\}$ (null set). Out of the 20 sensors, we set $\mathcal{J}_1 = \{5, 12, 16, 19\}$ as the set of informative sensors for FM 1 and $\mathcal{J}_2 = \{3, 7, 9, 19\}$ as the set of informative sensors for FM 2. The p^{th} sensor signal for the i^{th} system exhibiting failure mode k is generated using equation (20).

$$s_{i,p}^k(t) = -\frac{\theta_{i,p}^k}{\ln t} + \epsilon_{i,p}^k(t) \quad (20)$$

In this equation, $\epsilon_{i,p}^k(t) \sim N\left(0, (\sigma_k^p)^2\right)$ is a white noise process parameterized by $\sigma_k^p = \mu_k / SNR_p^k$, where SNR_p^k is the signal-to-noise for sensor p and failure mode k . To account for the correlation between the signal trends of the informative sensors and the underlying degradation process, we generate $\theta_{i,p}^k$ from the following conditional distribution $\theta_{i,p}^k \mid \theta_i^k \sim N\left(\mu_k \left(1 - \sqrt{1 - \rho_p^k}\right), (0.1)^2\right)$ such that the correlation, ρ_p^k , is uniformly

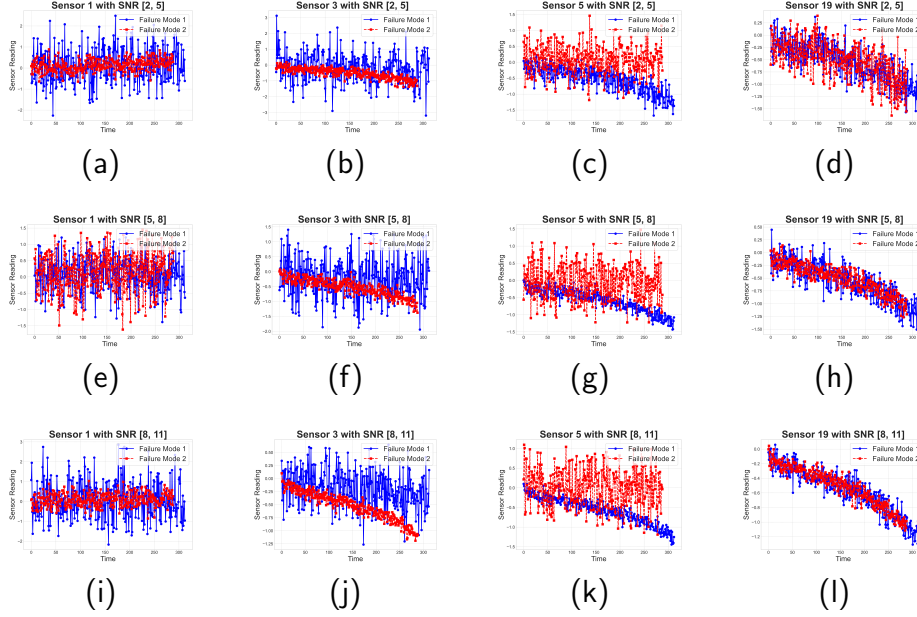


Figure 2: Case study 1 data: Signals in sensors 1, 3, 5, 19 (columns 1, 2, 3, 4 respectively) for FM 1 and 2 under different SNRs – [2, 5], [5, 8], and [8, 11] (rows 1, 2, 3 respectively)

sampled from the interval $[0.80, 0.99]$. The process for generating signals for the noninformative sensors is similar to that of the informative sensors, except the interval from which we sample ρ_p^k is $[0.1, 0.6]$. Finally, we randomly assign a sign to $\theta_{i,p}^k$ to allow for signals that increase or decrease in response to degradation.

In this simulation, we seek to test the robustness of our methodology to various levels of signal noise. Therefore, we generate three datasets, each with a unique interval from which to sample SNR_p^k . For $p \in \mathcal{J}_k$, SNR_p^k is sampled uniformly from [2, 5], [5, 8], and [8, 11] for datasets 1, 2, and 3, respectively. For $p \in \mathcal{N}_k$, SNR_p^k is sampled uniformly from [1, 3] for all three datasets. Figure 2 displays samples of our sensor signals in a 3x4 grid. Each row displays signals from four sensors (1, 3, 5, 19) for a particular signal-to-noise ratio. Sensor 1 is not informative for either failure mode so no discernible trend is present. Sensors 3 and 5 are informative for FM 2 and FM 1, respectively. For these sensors, one signal trends downward due to degradation while the other signal appears to resemble random noise. Finally, for sensor 19, the signal decreases in response to both failure modes.

Table 1: Tuning parameter selection for case study 1

SNR_p^k	[2,5]	[5,8]	[8,11]
λ	0.0466	0.0258	0.0258
α	1	0	0.25

6.2. Failure Mode Labeling and Sensor Selection

We analyze the ability of the MGR-ASGL model to accurately cluster the degradation signals into one of the two possible failure modes along with selecting the subset of informative sensors. We start by utilizing CA-FPCA as mentioned in 4.1 to extract features for each sensor separately. To determine the number of CA-FPC scores to retain, we use the 95% fraction of variance explained (FVE) criterion. For each cluster, we select the first q_p^k CA-FPC-scores whose eigenvalues sum to at least 0.95. Since the number of CA FPC scores to retain can vary for each cluster, we retain the maximum of q_p^k over both failure modes. For the remainder of this paper, we use 95% FVE criterion for determining the number of FPC scores, CA-FPC scores, and MFPC scores to retain. The CA-FPC scores serve as inputs to the MGR-ASGL model. Since this model has two tuning parameters, we utilize 5-fold cross-validation with $\lambda \in \{0.0050, 0.0258, 0.0466, \dots, 0.3792, 0.4000\}$ and $\alpha \in \{0.00, 0.25, 0.50, 0.75, 1.00\}$. We use minimum mean-squared error (minMSE) criterion, which selects the tuning parameters that minimize the mean-squared prediction error averaged over all folds. Table 1 displays the tuning parameter selection using both criteria over all three datasets. For each dataset and criterion, we fit the MGR-ASGL model using these tuning parameters.

We then evaluate the performance of the MGR-ASGL model on the three datasets. While clustering is an unsupervised learning task, we know the ground truth regarding the failure modes. Therefore, we evaluate the ability of the clustering algorithm to match the ground truth. Furthermore, we have predetermined which sensors are most informative and we would like to determine whether or not the MGR-ASGL selects these sensors. The results of this performance evaluation are shown in Table 2.

For all scenarios, the initial failure mode labels were determined randomly. Table II shows that for the lowest and the highest signal-to-noise ratios, the clustering algorithm was capable of achieving at worst 78.8% accuracy for a particular failure mode. The exception is the dataset [5,8], where

Table 2: MGR-ASGL performance for case study 1

SNR_p^k	FM	Accuracy	Sensors Selected
[2, 5]	1	0.800	1:3, 5, 7:9, 11:16, 18:20
	2	0.875	1, 3:4, 6:10, 13:14, 17:20
[5, 8]	1	0.506	1:7,9:12,14:20
	2	0.669	1:20
[8, 11]	1	0.825	1,3:20
	2	0.788	1:3,5:20

the algorithm has low accuracy at clustering. This is due to the tuning parameter combination resulting in minimal coefficient shrinkage that enabled the nonsignificant sensors to influence cluster assignments. A slightly larger λ value would decrease this error. For all three models, several sensors that are deemed "noninformative" were selected. This can be attributed to some of these sensors having high values of ρ_p^k relative to the specified range of [0.1,0.6]. However, simply reporting the sensors selected does not account for how informative they are. Table 3 reports the four sensors with the highest l_2 -norm of the regression coefficients associated with that sensor. Except for the [5,8] dataset, at least three of the four sensors with the largest l_2 -norm for each failure mode are elements of the set of informative sensors. This indicates that the MGR-ASGL model results in the informative sensors having larger regression coefficients (in magnitude) than the noninformative sensors. Given the selected sensors, we want to test the robustness of the online portion of the methodology to predict remaining life.

6.3. RUL Prediction

Each of the datasets consist of 80 test systems (40 from each failure mode). For each test system, we observe degradation up until the following life percentiles (in retrospect): 10%, 20%, 30%, 40%, 50%, 60%, 70%, 80%, and 90%. We smooth the training and the test signals using a bandwidth parameter of 0.5. Next, we perform MFPCA selecting the number using only the training systems that survived up to the observation time t^* corresponding to each life percentile. For a given test signal, we calculate its MFPC scores. The active failure mode is diagnosed by being assigned to the most frequent failure mode present in its closest $0.1N_{t^*}$ neighbors. Once

Table 3: l_2 -norms of four most informative sensors for FM1 & FM2

SNR_p^k	FM 1		FM 2	
	Sensor ID	l_2 -norm	Sensor ID	l_2 -norm
[2, 5]	5	1.809	9	1.667
	12	0.912	7	0.849
	16	0.604	19	0.303
	7	0.269	6	0.218
[5, 8]	5	1.137	9	1.153
	12	0.641	17	0.547
	17	0.500	19	0.537
	18	0.499	4	0.504
[8, 11]	12	1.982	9	2.150
	5	1.422	3	0.559
	16	1.016	19	0.540
	18	0.394	17	0.428

the active failure mode is identified, the MFPC scores of the test signals are updated and recomputed using the subset of training signals associated with the active failure mode. Next, we fit the weighted regression model and predict the RUL using the scores of the test signal. Prediction accurately is calculated retrospectively. We compute the “*Estimated Life*” as the current operating time plus the predicted RUL. A relative error is then computed using equation (21).

$$\text{Relative Error} = \frac{|\text{Estimated Life} - \text{Actual Life}|}{\text{Actual Life}} \times 100\% \quad (21)$$

The performance of our methodology on predicting RUL is shown in Figure 3. In this figure, the relative errors have a generally decreasing trend for all datasets, with the [8,11] dataset tending to have smaller relative errors on average. Furthermore, the variability appears to be much larger when making predictions early in the system’s life rather than later. Interestingly, the relative error increased for the [8,11] dataset when making predictions at 90% of the system’s life. This increase may be attributed to the increased influence of incorrectly clustered training samples affecting the RUL prediction. Since this dataset has less noise, the influence of clustering may be more

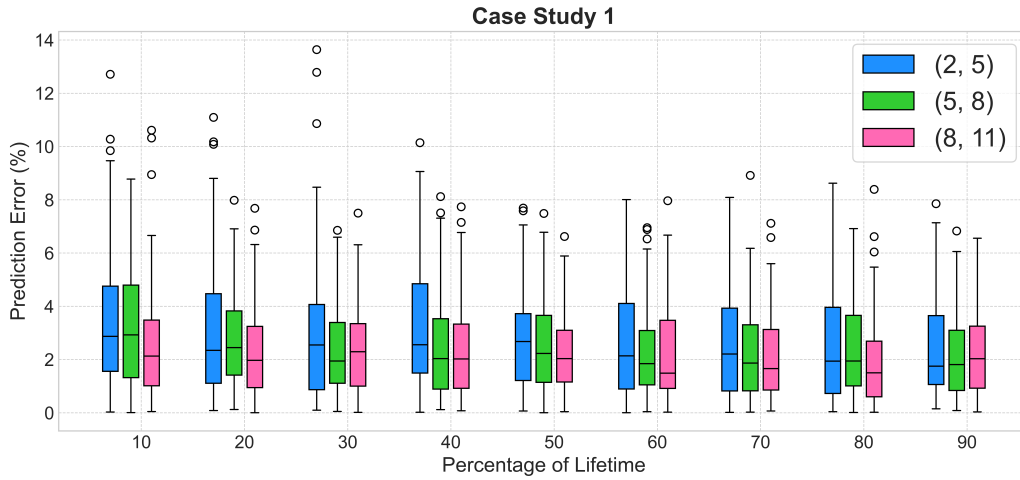


Figure 3: Prediction error (in %) for all test systems of case study 1 under three different SNRs i.e., [2, 5], [5, 8], and [8, 11]

pronounced compared to the noisier datasets, especially if training samples have been removed for failing before 90% of the monitored system’s lifetime.

7. Case Study 2: NASA Turbofan Engine Dataset

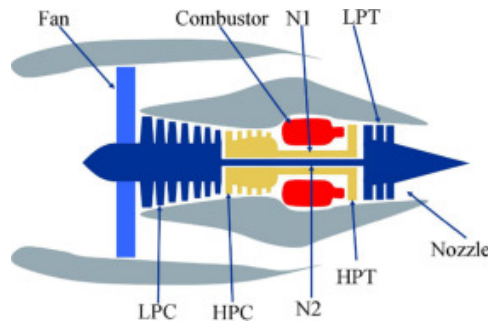


Figure 4: The system diagram used in Case Study 2 adapted from [44]

To further validate our methodology, we evaluate its performance on one of the Commercial Modular Aero-Propulsion System Simulation (C-MAPSS) datasets [44]. C-MAPSS is a simulation module that generates turbofan engine degradation datasets. Figure 4 displays a diagram of this turbofan engine. In this paper, we utilize *C-MAPSS-3*, which consists of both a training

Table 4: Sensors used in case study 2 (C-MAPPS-3 [44])

Sensor ID	Sensor Name	Functionality
1	T2	Total temperature at fan inlet
2	T24	Total temperature at LPC outlet
3	T30	Total temperature at HPC outlet
4	T50	Total temperature at LPT outlet
5	P2	Pressure at fan inlet
6	P15	Total pressure in bypass-duct
7	P30	Total pressure at HPC outlet
8	Nf	Physical fan speed
9	Nc	Physical core speed
10	epr	Engine pressure ratio (P50/P2)
11	Ps30	Static pressure at HPC outlet
12	phi	Ratio of fuel flow to Ps30
13	NRf	Corrected fan speed
14	Nrc	Corrected core speed
15	BPR	Bypass ratio
16	farB	Burner fuel-air ratio
17	htBleed	Bleed enthalpy
18	Nfdmd	Demanded fan speed
19	PCNfRdmd	Demanded corrected fan speed
20	W31	HPT coolant bleed
21	W32	LPT coolant bleed

and a test set. Both sets contain 100 observed engine failures caused by either fan degradation or high-pressure compressor degradation. Furthermore, both sets contain data from 21 sensors, which are listed in Table 4. The signals for these sensors are displayed in Figure 5. These sensors monitor the systems from a good-as-new state to engine failure. However, sensors 1, 5, 6, 10, 16, 18, and 19 contain little to no information and are thus removed from the analysis. While the dataset provides the potential causes of failure, it does not provide the failure labels. Furthermore, the test set consists of systems whose degradation is only partially observed along with their corresponding failure times. Therefore, our goal is to use our methodology to predict the remaining life of each testing unit following the final cycle at which their degradation was observed.

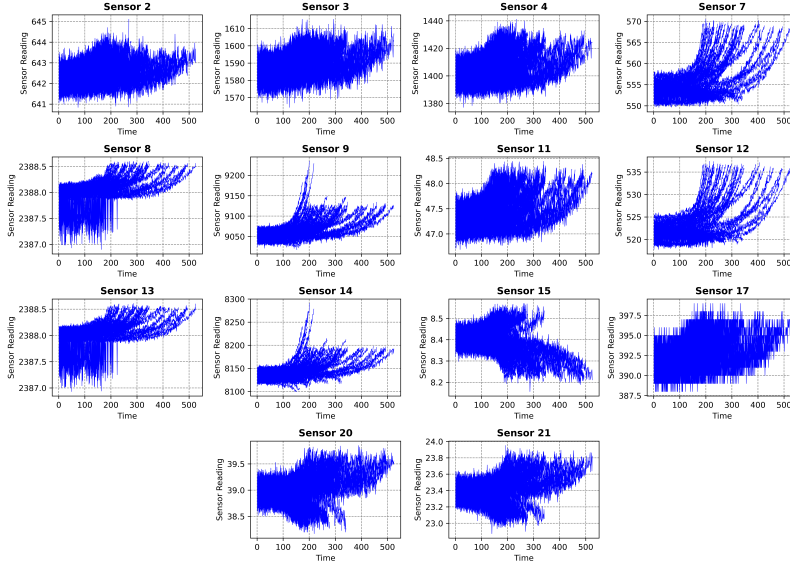


Figure 5: Raw sensor data used for offline step in case study 2. The data is inherently unlabeled i.e., failure modes are not known.

Our first step is to perform traditional FPCA on the signals for each sensor. We obtain initial failure mode labels for the training set by applying K-means clustering to all FPC-scores. Then, for each sensor, we apply K-means clustering to the FPC-scores associated with that sensor to obtain the covariate information needed to perform CA-FPCA. Following feature extraction, we use 3-fold cross-validation to determine (λ, α) . The range of values for these tuning parameters are identical to that of the simulation case study. The combination of tuning parameters that minimize the mean squared error across the three folds is $(\lambda_{MSE}, \alpha_{MSE}) = (0.1089, 1)$. Table 5 displays the l_2 -norms of the regression coefficients for each sensor. The sensors selected are those with positive l_2 -norms.

In addition to performing sensor selection, the MGR-ASGL model provides cluster labels for each observed failure. These labels are utilized for the online prediction portion of the methodology. For the online prediction step, we first smooth the degradation signals using 5-fold cross-validation to select the bandwidth parameter. After smoothing, we perform MFPCA on signals from the sensors selected across both failure modes to build our classifier. Then, we classify the failure mode based on the $0.1N_{t^*}$ nearest neighbors. Given this classification, we perform MFPCA on signals from the

Table 5: Sensor Selection for Case Study 2

Sensor ID	FM 1	FM2	Sensor ID	FM 1	FM 2
2	0.266	0	12	0	1.148
3	0.584	0	13	0.90	0
4	0.897	0.033	14	0.148	0.119
7	0	0.877	15	0.501	0
8	0.117	0	17	0.230	0.042
9	0.545	0.291	20	0	0.573
11	0	0	21	0.116	0.318

sensors selected for the classified failure mode. Finally, we perform Weighted Time-varying Functional Regression to regress $\ln TTF$ on the MFPC-scores using Leave-one-out cross-validation to select the tuning parameter.

Benchmarking: To analyze our methodology, we compare its performance to that of [32] (**Chehade et al. 2018**), whose methodology assumes knowledge of the failure modes but does not perform sensor selection (outside of removing the blank sensors), and [33] (**Li et al. 2023**), whose methodology assumes knowledge of a fraction of the training set and does perform sensor selection. Figure 6 displays the relative prediction error averaged over all test systems with RUL at most 100, 80, 60, 40, and 20 cycles. From this figure, our methodology becomes more accurate as the RUL decreases. Furthermore, our methodology is more accurate than both when making longer predictions. For test units whose RUL is at most 20, our accuracy is between that of [32] and [33]. Only at RUL at most 40, does our methodology perform worse than both. To further analyze our methodology, we refer to Figure 7, which displays boxplots showing the distribution of the relative prediction error for test units with remaining life in the following intervals: $[0, 25]$, $[26, 50]$, $[51, 75]$, $[76, 100]$, $[101, 125]$, $[126, 150]$. The results indicate that our methodology achieves a lower median relative error than [32] in all intervals while maintaining comparable variability. However, the variability for systems with RUL between 25 and 50 is higher for our methodology than for [32]. This indicates a targeted area for improvement of our methodology. However, the general trend is that sensor selection resulted in a more accurate RUL prediction than no sensor selection. Furthermore, we were capable of achieving more accurate RUL prediction than both methods from earlier in the systems’ lives despite not having information about the actual failure mode.

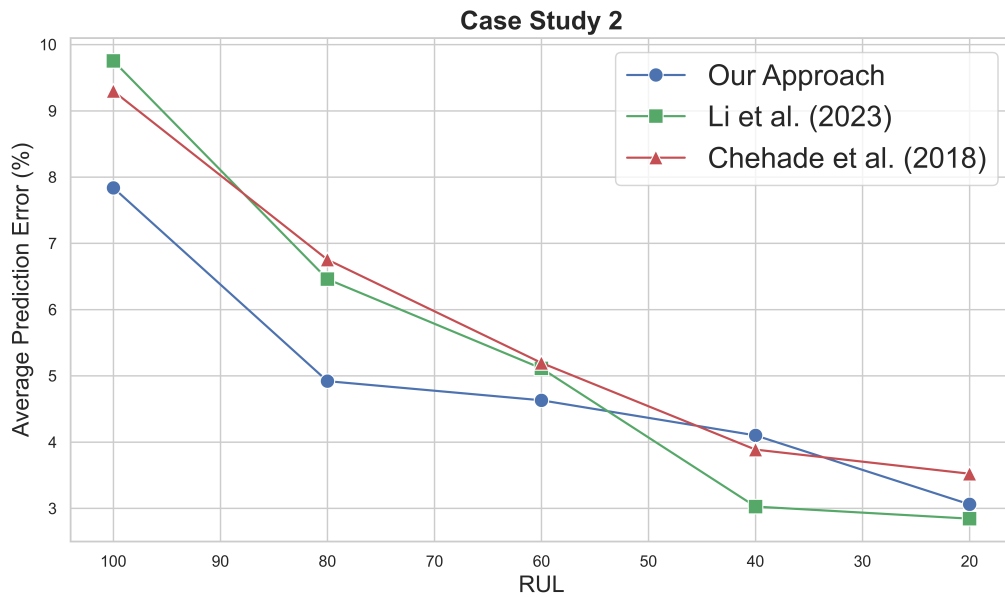


Figure 6: Average Prediction error (%) in case study 2 with comparison to [33], and [32]

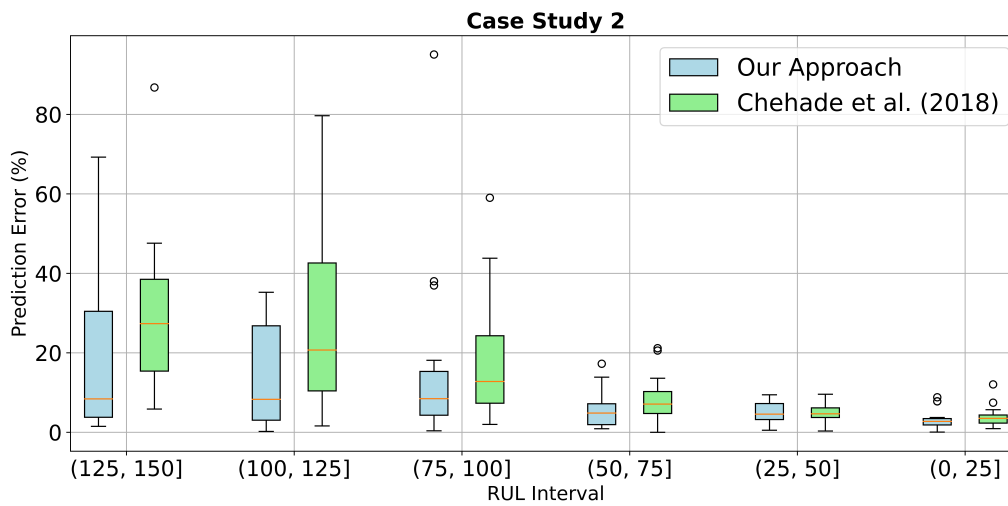


Figure 7: Prediction error (%) for different RUL intervals in case study 2 with comparison to [32]

8. Conclusion

In this paper, we present a methodology for predicting the RUL of systems with multiple failure modes using multiple sensors. This methodology consists of two phases: an offline phase and an online phase. Assuming that failure modes are mutually exclusive, the offline phase consists of a framework for diagnosing the observed failures in the training set and selecting an optimal subset of sensors for monitoring. In this framework, we utilize CAFPCA to capture the multiple failure modes exhibited by the sensor signals enabling the extraction of informative features. These features are used by our proposed EM algorithm to train the MGR-ASGL model which simultaneously diagnoses the training set failures and selects an optimal subset of informative sensors for each failure mode. In the online phase, we use MFPCA to fuse all the signals of the selected sensors into a parsimonious set of features to diagnose the failure mode for an actively degrading system. Then MFPCA is re-used to fuse the signals from informative sensors of the diagnosed failure mode for RUL prediction. RUL prediction is done using a time-varying weighted functional regression model.

To assess the performance of our methodology, we implemented it on two datasets – a) a simulated dataset and b) the NASA turbofan engine degradation dataset. For the simulated dataset, we tested the robustness of our methodology to various degrees of signal noise. We demonstrated that with a sufficiently high λ value, the clustering matches the actual clusters at an accuracy of about 80%. Furthermore, the most significant sensors occupied 3 of the top 4 slots with regard to l_2 -norm of regression coefficients. Finally, the methodology showed high accuracy with an average relative prediction error of no larger than 3, irrespective of the percentage of lifetime the prediction was performed.

In our real-world data case study, results show that our model makes early predictions more accurately than the two benchmarks while achieving comparable accuracy in later predictions. To achieve this, we identified 10 sensors to monitor the first failure mode while identifying 8 sensors to monitor the second failure mode. Our methodology removed one sensor completely. The region in which our methodology performed worst relative to the two baselines was when the RUL was between 25 and 50. A possibility for improvement would be to relax the assumption of a linear relationship between the $\ln TTF$ and the sensor signals. However, embedding a variable selection technique within a nonlinear regression model is an open topic in the litera-

ture. Therefore, the extension of this work to a nonlinear setting is a topic for future work.

Acknowledgments

This effort is supported by NASA under grant number 80NSSC19K1052 as part of the NASA Space Technology Research Institute (STRI) Habitats Optimized for Missions of Exploration (HOME) ‘SmartHab’ Project. Any opinions, findings, conclusions, or recommendations expressed in this material are those of the authors and do not necessarily reflect the views of the National Aeronautics and Space Administration.

References

- [1] J. Deutsch, D. He, Using deep learning-based approach to predict remaining useful life of rotating components, *IEEE Transactions on Systems, Man, and Cybernetics: Systems* 48 (1) (2018) 11–20. doi:10.1109/TSMC.2017.2697842.
- [2] H. Pei, X.-S. Si, C. Hu, T. Li, C. He, Z. Pang, Bayesian deep-learning-based prognostic model for equipment without label data related to lifetime, *IEEE Transactions on Systems, Man, and Cybernetics: Systems* 53 (1) (2023) 504–517. doi:10.1109/TSMC.2022.3185102.
- [3] N. Gebraeel, Sensory-updated residual life distributions for components with exponential degradation patterns, *IEEE Transactions on Automation Science and Engineering* 3 (4) (2006) 382–393. doi:10.1109/TASE.2006.876609.
- [4] Y. Zhang, Y. Yang, H. Li, X. Xiu, W. Liu, A data-driven modeling method for stochastic nonlinear degradation process with application to rul estimation, *IEEE Transactions on Systems, Man, and Cybernetics: Systems* 52 (6) (2022) 3847–3858. doi:10.1109/TSMC.2021.3073052.
- [5] X.-S. Si, W. Wang, C.-H. Hu, D.-H. Zhou, M. G. Pecht, Remaining useful life estimation based on a nonlinear diffusion degradation process, *IEEE Transactions on Reliability* 61 (1) (2012) 50–67. doi:10.1109/TR.2011.2182221.

- [6] L. A. Rodríguez-Picón, A. P. Rodríguez-Picón, L. C. Méndez-González, M. I. Rodríguez-Borbón, A. Alvarado-Iniesta, Degradation modeling based on gamma process models with random effects, *Communications in Statistics - Simulation and Computation* 47 (6) (2018) 1796–1810. doi:10.1080/03610918.2017.1324981.
- [7] W. Wang, A prognosis model for wear prediction based on oil-based monitoring, *Journal of the Operational Research Society* 58 (7) (2007) 887–893. doi:10.1057/palgrave.jors.2602185.
- [8] M. J. Mcghee, V. M. Catterson, B. Brown, Prognostic modeling utilizing a high-fidelity pressurized water reactor simulator, *IEEE Transactions on Systems, Man, and Cybernetics: Systems* 48 (5) (2018) 727–732. doi:10.1109/TSMC.2017.2662478.
- [9] C. Song, K. Liu, X. Zhang, A generic framework for multisensor degradation modeling based on supervised classification and failure surface, *IIEE Transactions* 51 (11) (2019) 1288–1302. doi:10.1080/24725854.2018.1555384.
- [10] Z. Li, K. Goebel, D. Wu, Degradation modeling and remaining useful life prediction of aircraft engines using ensemble learning, *Journal of Engineering for Gas Turbines and Power* 141 (041008) (Nov 2018). doi:10.1115/1.4041674.
URL <https://doi.org/10.1115/1.4041674>
- [11] P. Wen, S. Chen, S. Zhao, Y. Li, Y. Wang, Z. Dou, A novel bayesian update method for parameter reconstruction of remaining useful life prognostics, in: *2019 IEEE International Conference on Prognostics and Health Management (ICPHM)*, 2019, p. 1–8. doi:10.1109/ICPHM.2019.8819377.
- [12] L. Gu, Y. Zhou, Z. Zhang, H. Li, L. Zhang, Remaining useful life prediction using dynamic principal component analysis and deep gated recurrent unit network, in: *2021 Global Reliability and Prognostics and Health Management (PHM-Nanjing)*, 2021, p. 1–5. doi:10.1109/PHM-Nanjing52125.2021.9612895.
- [13] X. Fang, K. Paynabar, N. Gebrael, Multistream sensor fusion-based prognostics model for systems with single failure modes, *Reliability En-*

- gineering & System Safety 159 (2017) 322–331. doi:10.1016/j.ress.2016.11.008.
- [14] M. Kim, C. Song, K. Liu, A generic health index approach for multisensor degradation modeling and sensor selection, *IEEE Transactions on Automation Science and Engineering* 16 (3) (2019) 1426–1437. doi:10.1109/TASE.2018.2890608.
- [15] D. Wang, K. Liu, X. Zhang, A generic indirect deep learning approach for multisensor degradation modeling, *IEEE Transactions on Automation Science and Engineering* 19 (3) (2022) 1924–1940. doi:10.1109/TASE.2021.3072363.
- [16] N. Li, Y. Lei, N. Gebraeel, Z. Wang, X. Cai, P. Xu, B. Wang, Multi-sensor data-driven remaining useful life prediction of semi-observable systems, *IEEE Transactions on Industrial Electronics* 68 (11) (2021) 11482–11491. doi:10.1109/TIE.2020.3038069.
- [17] B. Wu, J. Zeng, H. Shi, X. Zhang, G. Shi, Y. Qin, Multi-sensor information fusion-based prediction of remaining useful life of nonlinear wiener process, *Measurement Science and Technology* 33 (10) (2022) 105106. doi:10.1088/1361-6501/ac7636.
- [18] N. Daroogheh, A. Baniamerian, N. Meskin, K. Khorasani, Prognosis and health monitoring of nonlinear systems using a hybrid scheme through integration of pfs and neural networks, *IEEE Transactions on Systems, Man, and Cybernetics: Systems* 47 (8) (2017) 1990–2004. doi:10.1109/TSMC.2016.2597272.
- [19] Q. Zhang, C. Hua, G. Xu, A mixture weibull proportional hazard model for mechanical system failure prediction utilising lifetime and monitoring data, *Mechanical Systems and Signal Processing* 43 (1) (2014) 103–112. doi:10.1016/j.ymsp.2013.10.013.
- [20] D. R. Cox, Regression models and life-tables, *Journal of the Royal Statistical Society. Series B (Methodological)* 34 (2) (1972) 187–220.
- [21] K. Monterrubio-Gómez, N. Constantine-Cooke, C. A. Vallejos, A review on competing risks methods for survival analysis (arXiv:2212.05157), arXiv:2212.05157 [stat] (Dec 2022).

- [22] X. Zhu, J. Yao, J. Huang, Deep convolutional neural network for survival analysis with pathological images, in: 2016 IEEE International Conference on Bioinformatics and Biomedicine (BIBM), 2016, p. 544–547. doi:10.1109/BIBM.2016.7822579.
- [23] E. Giunchiglia, A. Nemchenko, M. van der Schaar, Rnn-surv: A deep recurrent model for survival analysis, in: V. Kůrková, Y. Manolopoulos, B. Hammer, L. Iliadis, I. Maglogiannis (Eds.), Artificial Neural Networks and Machine Learning – ICANN 2018, Lecture Notes in Computer Science, Springer International Publishing, Cham, 2018, p. 23–32. doi:10.1007/978-3-030-01424-7_3.
- [24] G. Gupta, V. Sunder, R. Prasad, G. Shroff, Cresa: A deep learning approach to competing risks, recurrent event survival analysis, in: Q. Yang, Z.-H. Zhou, Z. Gong, M.-L. Zhang, S.-J. Huang (Eds.), Advances in Knowledge Discovery and Data Mining, Lecture Notes in Computer Science, Springer International Publishing, Cham, 2019, p. 108–122. doi:10.1007/978-3-030-16145-3_9.
- [25] P. Marthin, N. A. Tutkun, Recurrent neural network for complex survival problems, *Journal of Statistical Computation and Simulation* 0 (0) (2023) 1–25. doi:10.1080/00949655.2023.2176504.
- [26] P. Wang, Y. Li, C. K. Reddy, Machine learning for survival analysis: A survey, *ACM Computing Surveys* 51 (6) (2019) 110:1–110:36. doi:10.1145/3214306.
- [27] H. Li, W. Zhao, Y. Zhang, E. Zio, Remaining useful life prediction using multi-scale deep convolutional neural network, *Applied Soft Computing* 89 (2020) 106113. doi:10.1016/j.asoc.2020.106113.
- [28] O. O. Aremu, R. A. Cody, D. Hyland-Wood, P. R. McAree, A relative entropy based feature selection framework for asset data in predictive maintenance, *Computers & Industrial Engineering* 145 (2020) 106536. doi:10.1016/j.cie.2020.106536.
- [29] M. Kim, K. Liu, A bayesian deep learning framework for interval estimation of remaining useful life in complex systems by incorporating general degradation characteristics, *IISE Transactions* 53 (3) (2021) 326–340. doi:10.1080/24725854.2020.1766729.

- [30] R. Jiao, K. Peng, J. Dong, C. Zhang, Fault monitoring and remaining useful life prediction framework for multiple fault modes in prognostics, *Reliability Engineering & System Safety* 203 (2020) 107028. doi:10.1016/j.ress.2020.107028.
- [31] J. Xiong, J. Zhou, Y. Ma, F. Zhang, C. Lin, Adaptive deep learning-based remaining useful life prediction framework for systems with multiple failure patterns, *Reliability Engineering & System Safety* 235 (2023) 109244. doi:10.1016/j.ress.2023.109244.
- [32] A. Chehade, C. Song, K. Liu, A. Saxena, X. Zhang, A data-level fusion approach for degradation modeling and prognostic analysis under multiple failure modes, *Journal of Quality Technology* 50 (2) (2018) 150–165. doi:10.1080/00224065.2018.1436829.
- [33] H. Wu, Y.-F. Li, A multi-sensor fusion-based prognostic model for systems with partially observable failure modes, *IISE Transactions* 0 (ja) (2023) 1–21. doi:10.1080/24725854.2023.2222402.
- [34] C.-R. Jiang, J.-L. Wang, Covariate adjusted functional principal components analysis for longitudinal data, *The Annals of Statistics* 38 (2) (2010) 1194–1226.
- [35] K. Karhunen, Über lineare Methoden in der Wahrscheinlichkeitsrechnung, Kirjapaino oy. sana, 1947, google-Books-ID: bGUUAQAIAAJ.
- [36] F. Yao, H.-G. Müller, J.-L. Wang, Functional data analysis for sparse longitudinal data, *Journal of the American Statistical Association* 100 (470) (2005) 577–590. doi:10.1198/016214504000001745.
- [37] N. Städler, P. Bühlmann, S. van de Geer, L1-penalization for mixture regression models, *TEST* 19 (2) (2010) 209–256, arXiv:1202.6046 [stat]. doi:10.1007/s11749-010-0197-z.
- [38] K. P. Murphy, *Machine learning: a probabilistic perspective*, MIT press, 2012.
- [39] R. Tibshirani, Regression shrinkage and selection via the lasso, *Journal of the Royal Statistical Society. Series B (Methodological)* 58 (1) (1996) 267–288.

- [40] W. S. Cleveland, Robust locally weighted regression and smoothing scatterplots, *Journal of the American Statistical Association* (Apr 2012).
URL <https://www.tandfonline.com/doi/abs/10.1080/01621459.1979.10481038>
- [41] H.-G. Müller, Y. Zhang, Time-varying functional regression for predicting remaining lifetime distributions from longitudinal trajectories, *Biometrics* 61 (4) (2005) 1064–1075.
- [42] X. Fang, R. Zhou, N. Gebraeel, An adaptive functional regression-based prognostic model for applications with missing data, *Reliability Engineering & System Safety* 133 (2015) 266–274. doi:10.1016/j.ress.2014.08.013.
- [43] T. Strutz, *Data fitting and uncertainty: A practical introduction to weighted least squares and beyond*, Vol. 1, Springer, 2011.
- [44] A. Saxena, K. Goebel, D. Simon, N. Eklund, Damage propagation modeling for aircraft engine run-to-failure simulation, in: *2008 International Conference on Prognostics and Health Management*, 2008, p. 1–9. doi:10.1109/PHM.2008.4711414.